Stall Dynamics of a Cross-Flow Turbine

Robert J. Cavagnaro*
University of Washington,
Mechanical Engineering
Seattle, WA, USA

Brian Polagye
University of Washington,
Mechanical Engineering
Seattle, WA, USA

*Corresponding author: rcav@uw.edu

1. INTRODUCTION

As development of hydrokinetic turbines advances, increasing focus is being placed on developing control strategies to meet a number of goals. These may be formulated to optimize performance, reduce loading, or maintain power at a constant value. The task of developing a controller invariably depends on knowledge of or the ability to identify a reliable model of system dynamics and stability. Such a model is necessary for numerical simulation of a turbine and controller. A dynamic system representing a hydrokinetic turbine can quickly grow in complexity when considering variants with many degrees of freedom (e.g., variable pitch, active yaw, gearing, variable speed generator). Dynamics are further complicated by the fact that a turbine's output depends on a nonlinear relationship with an uncontrollable turbulent hydrokinetic resource (i.e., river, tidal channel, ocean current). However, the order of complexity can be reduced to a single degree of freedom (angular position of the turbine) when studying fixed-pitch, direct drive, cross-flow designs.

A fixed-pitch turbine's performance is a function of its tip-speed ratio (λ)

$$\lambda = \frac{\omega R}{U_\infty} \tag{1}$$

where ω, R, and U_∞ denote rotation rate, radius, and free-stream speed, respectively. Mechanical efficiency, or coefficient of performance (C_P) is the ratio of mechanical power output to the kinetic power of the inflow,

$$C_P = \frac{\tau_h \omega}{\frac{1}{2}\rho A U_\infty^3} \tag{2}$$

in which τ_h is the torque developed by the turbine, ρ the density of water, and A the rotor projected area (product of length (L) and diameter (D) for cross-flow turbines). Torque relative to fluid forcing can similarly be parameterized with λ as a non-dimensional coefficient (C_Q)

$$C_Q = \frac{\tau_h}{\frac{1}{2}\rho A R U_\infty^2} = \frac{C_P}{\lambda}. \tag{3}$$

The relationship between λ and C_P intuitively points out favorable operating conditions; in many instances it is desirable to operate a turbine near the peak identified in the curve. Additionally, characterization by (3) provides valuable information on conditions to avoid; it describes a limit of stability, though not in as intuitive a manner as the performance maximum.

Change in a fixed-pitch cross-flow turbine's rotation rate can be modeled with a first-order, nonlinear ODE

$$\dot{\omega} = \frac{1}{J}(\tau_h - B\omega - \tau_c) \tag{4}$$

where J is the rotational moment of inertia of the turbine and power take-off (PTO), B is a damping coefficient, and τ_c is control torque, or the loading provided by the PTO or other mechanical means. The formulation of (4) does not account for PTO stiffness or the effects of added mass, which may be significant if angular acceleration is high (e.g., when using a controller to rapidly change the speed of the rotor).

The practice of controlling a turbine by braking (supplying τ_c) is known as stall regulation or torque control [1]. Challenges to this method of control may be a turbine's capacity to catastrophically stall (cease rotation) during operation at low λ, as well as increased thrust loading and emergency stopping hazards while operating at high λ. An analytical explanation for system stall (as distinct from the hydrodynamic phenomenon of dynamic stall present in the course of normal rotation) under torque control is developed in the following section. This is followed by the description of a laboratory experiment to characterize the behavior of a stalling turbine. Results of this analysis and experiment are subsequently described and discussed.

2. METHODS

2.1 System Stall Dynamics

Previous studies analyzing the dynamics of wind turbines with performance characteristics similar to hydrokinetic turbines have linearized (4) as a stage in controller development and note stable operation cannot be maintained at λ lower than a critical value (λ_c) as-
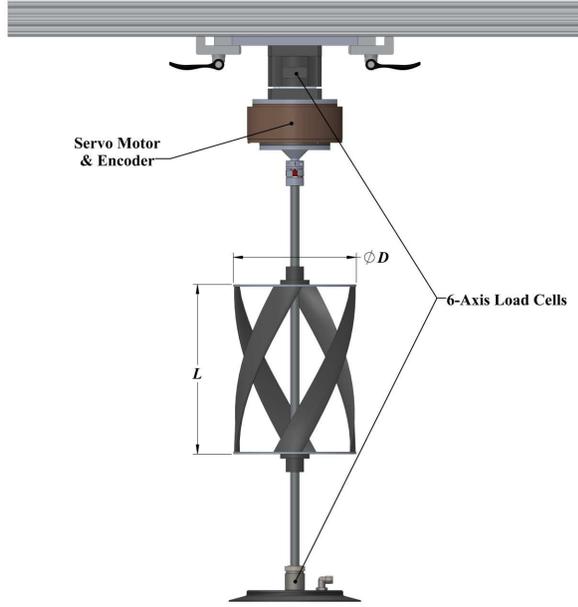
Figure 1: Turbine and test apparatus.

Figure 2: Characteristic performance and torque curves at 1 m/s.

sociated with peak C_Q [2],[3]. Indeed, linear analysis indicates instability of a turbine at this point due to antiphase response [4]. However, this mathematical explanation lacks an intuitive connection to the underlying hydrodynamics.

An analytical determination of the conditions in which a stall-regulated turbine becomes unstable can be performed utilizing knowledge of $C_Q(\lambda)$ as characterized during steady-state operation. A characteristic torque curve is related to a characteristic performance curve ($C_P(\lambda)$) through (3), both of which have been obtained for a laboratory-scale cross-flow helical fixed-pitch hydrokinetic turbine (Figure 1) whose parameters are described in Table 1. The curves were produced from measurements of shaft torque and prescribed rotation rate of a coupled servomotor (speed control) for 30 s in a recirculating flume set to provide U_∞ at 1 m/s. Further details of the experimental apparatus are given in [5]. Inflow was monitored with an acoustic Doppler velocimeter (ADV, Nortek Vector) positioned at the turbine centerline $5D$ upstream of the turbine. The points on the curves shown in Figure 2 represent average values for C_P and C_Q under stationary conditions such that, nominally, $\tau_h = B\omega + \tau_c$. Cubic polynomials have been fit to the curves in order to analytically evaluate $\tau_h(\lambda, U_\infty)$ as

$$\tau_h = (a\lambda^3 + b\lambda^2 + c\lambda + d)\rho LR^2 U_\infty{}^2, \quad (5)$$

with a, b, c, d being empirical constants. The curves map stable operating states that the speed-controlled turbine, on average, converges to. A cubic polynomial is the least complicated function able to describe the global maximum in performance with no local extrema and the asymmetry in performance around the maximum. The following analysis holds for any functional representation of $C_Q(\lambda)$ that satisfies these conditions.

The relationship between (4) and (5) indicates a tur-

bine operating at a steady ω with finite and nonzero J will experience an increase in τ_h subject to an increase in U_∞ and a decrease in τ_h subject to a decrease in U_∞ under constant resistive torque (τ_c). Step changes in U_∞ ultimately result in step changes in ω, with a final speed obtained when the turbine returns to a condition in which hydrodynamic torque is balanced against control torque and damping (friction losses). Given a known initial state ($\lambda_i, U_{\infty,i}, \tau_{h,i}$), it is possible to determine a final state ($\lambda_f, U_{\infty,f}, \tau_{h,f}$) that is the result of a change in U_∞ by solving (5) for λ. As system stall is observed during deceleration, changes in inflow speed considered herein are assumed negative, such that $U_{\infty,f} < U_{\infty,i}$.
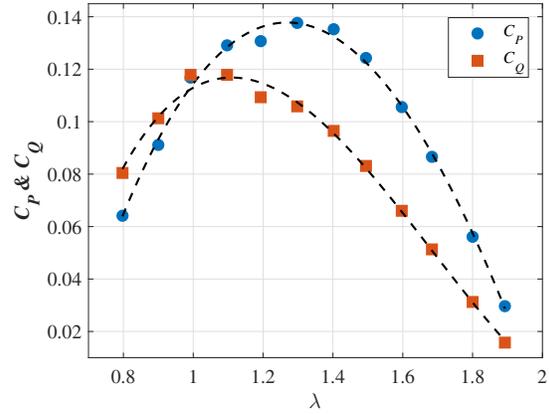
A valid solution to (5) (real-valued, in range where C_Q is defined) exists for a decrease from $U_{\infty,i}$ under the following conditions: 1. the turbine is perturbed from $\lambda_i > \lambda_c$, and 2. $U_{\infty,f}$ exceeds a certain threshold. Condition 1 exists because the turbine cannot decelerate to a state that produces higher torque when U_∞ decreases if it starts at $\lambda_i \leq \lambda_c$; the resistive torque command held at the initial state will always be higher than $\tau_{h,f}$. For condition 2, the magnitude of drop in U_∞ a turbine perturbed from λ_i can withstand (i.e., settle at another stable rotation rate, ω_f) increases as λ_i is increased; intuitively, the further to the right on the $C_Q(\lambda)$ curve the turbine begins at, the more stable operating states are available to it.

Maximum possible step decrease in U_∞ as a function of λ_i and $U_{\infty,i}$ was analytically evaluated for the laboratory-scale turbine. This was accomplished numer-

ically by setting initial conditions, perturbing the system with a drop to $U_{\infty,f}$, and searching for valid solutions to (5) that minimized the difference between $\tau_{h,f}$ and $B\omega_f + \tau_c$.

2.2   System Stall Experiments

Experiments to quantify the operating and environmental conditions of a turbine undergoing system stall were conducted with the same device whose performance is described by Figure 2. The turbine was allowed to accelerate to a freewheel state (highest natural λ achievable) while the free-stream velocity was maintained at 1 m/s. Subsequently, the servomotor acting as the turbine PTO was commanded to enact a τ_c predetermined to decelerate the rotor to its critical speed, λ_c. This level of resistive torque was maintained until the turbine experienced complete stall or failed to stall within 60 s. The progression from operating at freewheel to reaching a rotation rate of 0 is referred to as a stall event. 288 stall events were carried out to create a robust dataset of conditions and a statistical distribution of time the turbine was able to maintain stable rotation before stalling. Forces acting on the turbine were measured with a 6-axis load cell, while angular position was monitored with an encoder. The three components of inflow velocity were measured using analog output from the ADV $5D$ upstream of the rotor. Data streams were sampled at 1000 Hz.

The homogeneity of the realizations and distinct modes of operation (e.g., bringing the turbine to λ_c, stable rotation) enabled the use of a cluster analysis method to objectively quantify the duration of stable operation at λ_c. This 'stable' time was systematically determined using a k-means classification algorithm implemented in MATLAB [6]. Five clusters were selected, as this resulted in grouping of the stall event into regions that qualitatively align with the known physically significant modes.

Measurements from the ADV were used to correlate flow conditions with ω during stall events. Due to the instrument's position upstream of the turbine, Taylor's frozen field hypothesis was employed to account for advection time of turbulent structures [7]. ADV measurements were de-spiked to remove spurious data [8]. Time series of inflow speed magnitude were smoothed with a moving average filter with a window size of 500 samples (0.5 s) to reduce high-frequency content. Correlation coefficient between ω and U_∞ was calculated to quantify how well the turbine's rotation rate tracks changes in inflow conditions. Turbulence intensity, defined as

$$I_U = \frac{\sigma_U}{\langle U_\infty \rangle} \tag{6}$$

where σ_U is the standard deviation and $\langle U_\infty \rangle$ is the mean of inflow speed, was also calculated. These quantities were compared between cases where system stall occurred 20 s - 40 s after test initiation and cases where the turbine did not stall after 60 s. It was hypothesized ω and U_∞ should be well-correlated, with a distinct observed decrease in U_∞ preceding system stall.
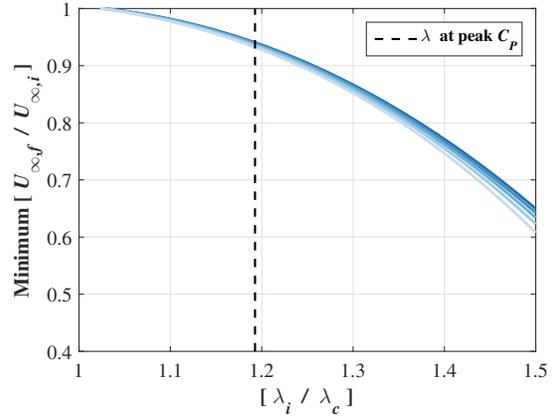
3.   RESULTS

Figure 3: Critical ratio of final to initial speeds given initial λ. Darker lines indicate larger $U_{\infty,i}$.
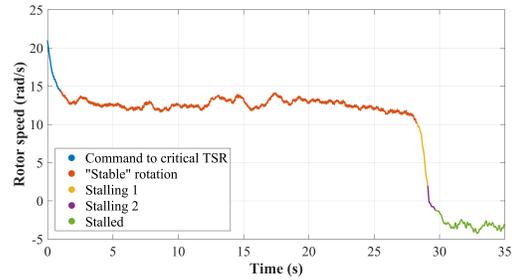

Figure 4: Time series of turbine rotation rate during stall event clustered into distinct regions.

3.1   Conditions Leading to Stall

The maximum sustained drop in U_∞ the turbine is capable of withstanding before system stall is shown to depend on both initial λ and U_∞ (Figure 3); distance from λ_c and a lower $U_{\infty,i}$ are the most stable conditions the turbine can operate under. However, while operating at peak C_P under constant torque control, this turbine can only withstand a sustained drop in inflow speed to roughly 90% of its initial value before system stall is probable. Turbulent gusts of this magnitude would be expected to occur during field operations [9]. Increased separation between λ at peak C_P and λ_c may be achieved with a turbine with a "flatter" characteristic curve near peak C_P (i.e., $\frac{dC_P}{d\lambda}$ lower). However, separation may decrease for a turbine operating at overall higher λ, which would be typical of cross-flow turbines with lower solidity.

3.2   Experimental Results

Stall events were successfully subdivided into five distinct regions using k-means classification. These identify when the turbine is brought to λ_c, stable operation at λ_c, a convex region of stalling, a concave region of stalling, and after the turbine has fully stalled. A time series of ω coded by these distinct portions of a typical stall event is shown in Figure 4.

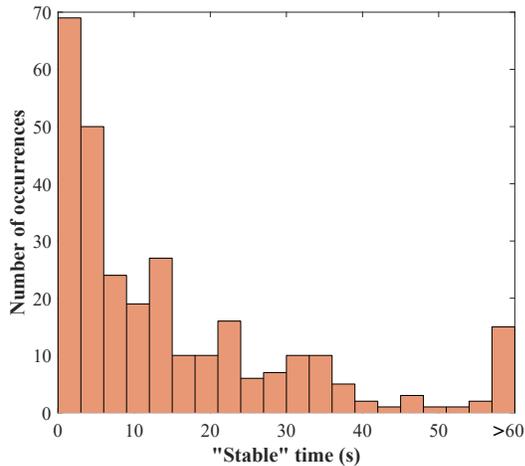The turbine is capable of maintaining operation at

Figure 5: Distribution of time classified as 'stable'.

Figure 6: Phase-averaged torque at λ_c for turbine regulated with speed control over 60 rotations.

λ_c for a range of time before system stall from stalling nearly instantly (the most probable outcome) to not stalling within 60 s. The median time classified as 'stable' is 9 s. The distribution of stable time before stall is shown in Figure 5. Average λ of this region is 1.09, in agreement with the predicted λ_c associated with maximum C_Q. Realizations counted in the final bin are expected to extend the distribution tail.

The correlation coefficient between ω and U_∞ is 0.33 for cases where stall occurred between 20 s and 40 s after test initiation and 0.37 for cases where the turbine did not stall. Turbulence intensity averages 5% for stalling cases as well as non-stalling cases. Mean inflow speed is nearly identical for all cases. Lower correlation for the stalling instances and no statistical differences in inflow conditions between cases indicate no distinct events in the measured inflow time series are definitively culpable for the onset of system stall.

4.   DISCUSSION AND CONCLUSIONS

An explanation for why system turbine stall occurs at λ corresponding to the peak of the $C_Q(\lambda)$ curve under torque control is presented. This argument considers sustained change in inflow speed and its effects on the turbine's ability to produce sufficient torque at a final state to maintain stable rotation. The method does not consider the effects of rapid fluctuations in inflow speed and the turbine having finite response time due to inertia. Under these more realistic conditions, the turbine would be more robust from system stall resulting from a deficit in inflow speed. These factors likely contributed to the wide range of time a laboratory-scale turbine was shown able to maintain its critical tip-speed ratio before system stall. The results are specific to the turbine and experimental conditions described; applicability to other turbine designs is not implied, but could be studied in future work. Additionally, at larger scale and with higher inertia, a turbine system becomes less susceptible to unintended changes in rotation rate. However, the method is useful for showing an arbitrary cross-flow
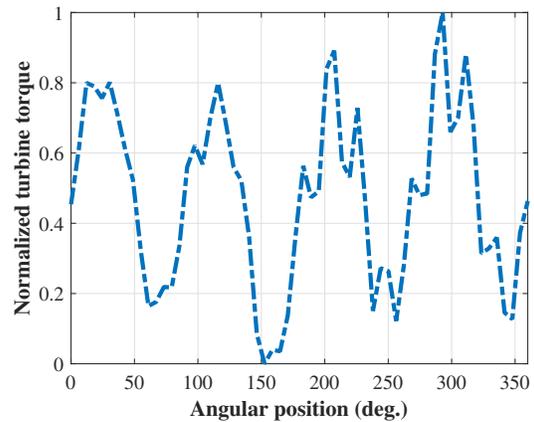
turbine's susceptibility to system stall when it operates near peak efficiency.

Correlation between upstream measurements of U_∞ and ω is relatively weak. Utilizing a point measurement of inflow which is often not homogeneous over the turbine projected area may not be sufficient to represent conditions leading to system stall. Additionally, cross-flow turbine power output and thus ability to produce torque is a strong function of the angular position of the rotor blades for straight-bladed designs [5]. Though to a lesser degree, this is true of helical turbines under speed control as well, with τ_h varying with rotor position, as shown in Figure 6. This indicates interactions between flow structures and the turbine at the blade level may contribute to system stall; the turbine might encounter slower flow at the "wrong" point in its rotation leading to an unsustainable drop in torque. Nonetheless, an accurate estimate of λ during field operation would aid in system stall characterization and avoidance.

Future work investigating conditions leading up to and during system stall will include analysis of particle image velocimetry taken directly upstream of the turbine. It is hypothesized that the ability to resolve larger coherent flow structures interacting with the turbine will enable stronger inferences to be drawn between the turbine's state and flow it is interacting with.

Designers of PTO systems for hydrokinetic turbines are actively investigating hardware and control strategies to operate more effectively in the regime slower than λ at maximum C_P [10]. The methods and results of this work will help in understanding the risks and limitations of operating a turbine in this 'underspeed' region.

5.   ACKNOWLEDGEMENTS

pany and Brian Fabien at the University of Washington for initial discussions on this topic.

6.   REFERENCES

[1] Manwell, J. F., McGowan, J. G., and Rogers, A. L., 2010. *Wind energy explained: theory, design and application*. John Wiley & Sons.

[2] Novak, P., Ekelund, T., Jovik, I., and Schmidtbauer, B., 1995. "Modeling and control of variable-speed wind-turbine drive-system dynamics". *IEEE Control Systems Magazine,* **15**(4), pp. 28–38.

[3] Bianchi, F. D., Battista, H., and Mantz, R. J., 2007. *Wind Turbine Control Systems: Principles, Modelling, and Gain Scheduling Design*. Springer-Verlag Limited, London, UK.

[4] Cavagnaro, R. J., 2014. "Impact of Turbulence on the Control of a Hydrokinetic Turbine". In International Conference on Ocean Energy.

[5] Strom, B., Brunton, S., and Polagye, B., 2015. "Consequences of Preset Pitch Angle on Cross-Flow Turbine Hydrodynamics". In Proceedings of the 11th European Wave and Tidal Energy Conference, no. 4, pp. 08D2–4–1:9.

[6] MATLAB, 2015. *Statistics and machine learning toolbox version 10.1 (R2015b)*. The MathWorks Inc., Natick, Massachusetts.

[7] Taylor, G. I., 1937. "The Statistical Theory of Isotropic Turbulence". *Journal of the Aeronautical Sciences,* **4**(8), pp. 311–315.

[8] Mori, N., Suzuki, T., and Kakuno, S., 2007. "Noise of Acoustic Doppler Velocimeter Data in Bubbly Flows". *Journal of Engineering Mechanics,* **133**(1), pp. 122–125.

[9] Thomson, J., Polagye, B., Durgesh, V., and Richmond, M. C., 2012. "Measurements of turbulence at two tidal energy sites in puget sound, WA". *IEEE Journal of Oceanic Engineering,* **37**(3), July, pp. 363–374.

[10] Djebarri, S., Charpentier, J., Sciuller, F., and Benbouzid, M., 2015. "Influence of Fixed-Pitch Tidal Turbine Hydrodynamic Characteristic on the Generator Design". In Proceedings of the 11th European Wave and Tidal Energy Conference, pp. 08A2–2–1:10.